Egyptian Journal of Petroleum (2016) 25, 171–181

HOSTED BY

ELSEVIER

Egyptian Petroleum Research Institute

Egyptian Journal of Petroleum

www.elsevier.com/locate/egyjp
www.sciencedirect.com

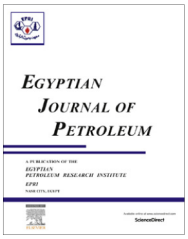

FULL LENGTH ARTICLE

Mn(II) removal from aqueous solutions by Co/Mo layered double hydroxide: Kinetics and thermodynamics

A.A. Bakr [a,1], M.S. Mostafa [b,*], E.A. Sultan [b,2]

[a] Egyptian Petroleum Research Institute (EPRI), Department of Analysis and Evaluation, Nasr City, Cairo 11727, Egypt
[b] Egyptian Petroleum Research Institute (EPRI), Department of Refining, Nasr City, Cairo 11727, Egypt

Received 15 February 2015; revised 31 March 2015; accepted 7 April 2015
Available online 17 December 2015

KEYWORDS

Water treatment;
Co/Mo-LDH;
Kinetics;
Mn(II) removal;
Thermodynamics

Abstract This paper deals with the experimental investigation related to the Mn(II) removal from aqueous solutions by the adsorption onto a synthesized Co/Mo layered double hydroxide (Co/Mo-LDH). The adsorption behavior was studied as a function of initial Mn(II) concentration (40–145 mg/L), contact time (15–90 min), solution pH (2–9) and adsorbent mass (0.05–0.35 g per 1.0 L). All adsorption processes were rapidly carried out at different temperatures (298, 308 and 318 K) and constant stirring rate 160 rpm. The results showed that the Co/Mo-LDH is a very promising material for removing of Mn(II) from the aqueous solutions. Particularly, the solution pH range of 4–7 has the most significant effect on the adsorption capacity. The results revealed that the maximum adsorption capacities were 20.2, 26.75 and 38.1 mg/g from the initial Mn(II) concentration (145 mg/L) at pH 5, adsorbent mass (0.2 g/1.0 L), and contact time (60 min) at different temperatures, 298, 308 and 318 K, respectively. The adsorption kinetics data are well fitted by the pseudo-second-order model, while the adsorption isotherms data were better fitted by the Langmuir equation. Also, this paper discusses the thermodynamic parameters of the adsorption and the results demonstrate that the adsorption process is spontaneous and endothermic.

1. Introduction

Manganese can be found in natural waters in its most reduced and soluble form, the Mn(II) ion and in the oxidized form MnO_2 (pyrolusite), respectively. If not oxidized, Mn(II) ions can easily escape through water treatment processes and can gradually be oxidized to insoluble manganic dioxide MnO_2 in the distribution system causing several problems such as water discoloration, metallic taste, odor, turbidity, biofouling and corrosion, staining of laundry and plumbing fixture [1].

* Corresponding author. Mobile: +20 1114502512 (M.S. Mostafa).
E-mail addresses: als_water@yahoo.com (A.A. Bakr), alphaalumina@yahoo.com (M.S. Mostafa), elsayedsultanepri@yahoo.com (E.A. Sultan).
[1] Mobile: +20 1227135228 (A.A. Bakr).
[2] Mobile: +20 1150016110 (E.A. Sultan).

Peer review under responsibility of Egyptian Petroleum Research Institute.

http://dx.doi.org/10.1016/j.ejpe.2015.04.002

Abbreviations

q_t	amount of adsorption capacity q_t (mg/g)	n	heterogeneity factor related to sorption intensity
q_e	equilibrium adsorption capacity, mg/g	k_1	pseudo-first-order rate constant for the adsorption process
C_0	initial concentration, mg/l	k_2	pseudo-second-order rate constant for the adsorption process
C_t	concentration after time t, mg/l	$\Delta G°$	Gibbs free energy for the adsorption process, kJ mol^{-1}
m	mass of the adsorbent, g	$\Delta H°$	enthalpy change for the adsorption process, kJ mol^{-1}
v	volume of solution, L	$\Delta S°$	entropy change for the adsorption process, kJ mol^{-1} K^{-1}
C_e	equilibrium adsorption concentration, mg/l	R	ideal gas constant, kJ mol^{-1} K^{-1}
K_L	Langmuir constant related to the sorption capacity, L/mg	T	temperature, K
b	Langmuir constant related to the energy of adsorption, mg/g		
K_F	Freundlich constant related to sorption capacity, L/mg		

For high intake manganese having adverse neurotoxic health effect, World Health Organization (WHO) recommends guideline value of 0.4 mg/L to protect against neurological damage [2]. European Union (EU) and the Environmental Protection Agency (EPA) have established the level of 0.05 mg/L for manganese [3,4]. So if concentrations are higher than these standards, then water must be treated before using it for drinking purposes. The excessive concentrations of Mn will result in metallic taste in water, staining of different products like clothes, paper and plastics [5]. Manganese can also cause build up in pipelines, water heaters and pressure tanks. The deposition of manganese in the distribution systems can cause reduction of pipe diameter and eventually clogging of pipe will take place [6].

Oxidation and precipitation is the most common method to remove Mn(II). Such method is based on the Mn(II) oxidation to its insoluble manganic dioxide, followed by clarification and/or filtration. Manganic dioxide is also found to adsorb the manganese ion which can be progressively oxidized with time [7]. Encouraging results for manganese removal have also been obtained by GAC adsorption [8] and biological processes [9,10], with removal up to 95%.

Nano-adsorbents are quite efficient for the fast adsorption of heavy-metal ions and organic molecules from aqueous solutions because of their high specific surface areas and the absence of internal diffusion resistance [11]. Layered double hydroxides (LDHs) are a class of nanostructured inter-layer anionic clays [12] and constitute a class of lamellar ionic compounds containing a positively charged layer and exchangeable anions in the interlayer [13].

While, the ordinary LDH is usually prepared from divalent and trivalent cations, the Co/Mo-LDH from bivalent and hexavalent cations was prepared as a new type of LDH [14]. This type of novel LDH nanoparticles was applied to the Fe(II) removal from aqueous solutions. Thereafter, the kinetics and thermodynamics of Fe(II) removal by Co/Mo-LDH were studied [15].

The objectives of the present study are synthesis of Co/Mo $(CO_3)^{2-}$-LDH nanoparticles, applying them for Mn(II) removal from aqueous solutions, determining the adsorption rate and capacity and thereafter, studying the kinetics and thermodynamics parameters of the adsorption processes.

2. Materials and methods

2.1. Materials

All chemicals with a purity of greater than 99.9% were purchased as follows: Manganese chloride ($MnCl_2 \cdot 4H_2O$) was purchased from Loba Chemie Co., anhydrous ($MoCl_5$), $CoCl_2 \cdot 6H_2O$, and ammonium carbonate $(NH_4)_2CO_3$ were purchased from Sigma–Aldrich (Germany) and NH_4OH (34%) was purchased from Merck Germany.

2.2. Preparation of Co/Mo-LDH

The method of Co/Mo$(CO_3)^{2-}$-LDH preparation was previously published [14]. In typical synthesis, a controlled co-precipitation method is applied based on increasing the rate of addition of NH_4OH and $(NH_4)_2CO_3$ into the Co and Mo cations at 60 °C. A solution A, 59 mmol of $MoCl_5$ and $CoCl_2.6H_2O$ with Co/Mo molar ratio of 0.25, was first prepared in 100 ml de-ionized water, while solution B was prepared from NH_4OH (10 mmol) and $(NH_4)_2CO_3$ (20 mmol) in 50 ml de-ionized water. Then solution B was gradually added into solution A successively till reaching a pH of about 9 with adjusted rate of addition to be through an aging time of 24 h at 60 °C under vigorous stirring. Finally, the formed puffy precipitate was filtered, washed with de-ionized water till the negative Cl ions are removed and dried at 60 °C overnight.

2.3. Characterization of Co/Mo-LDH

Here three main analytical techniques are presented for the prepared Co/Mo-LDH with respect to the Mn(II) adsorption process because the sample was previously proofed, tested and published as will be referenced in the preparation part. The XRD powder diffraction patterns have been performed with Bruker AXS-D8 Advance (Germany) using nickel filtered copper radiation (λ = 1.5405 A) at 60 kV and 25 mA with scanning speed of 8° in 20 min^{-1} over diffraction angle range. Fourier transfer infrared (FT-IR) spectra were recorded on ATI Mattson Genesis series (KBr disk method) apparatus, Model 960 M009 series. While the surface morphologies of

the prepared samples were analyzed by scanning electron microscope (SEM) using JEOL 5300 SEM instrument (Japan).

2.4. Adsorption method

The manganese Mn(II) stock solution concentration of 195 mg/L was prepared by dissolving Manganese chloride ($MnCl_2 \cdot 4H_2O$, Loba Chemie) in distilled water. The working Mn(II) solution concentration ranging from 40 to 145 mg/L for all experiments was freshly prepared from the stock solution. Standard acid (0.01 M HNO_3) and base solutions (0.125 M NaOH) were used for pH adjustments at pH 2, 3, 4, 5, 6, 7, 8 and 9. The pH of the solution was measured with a pH meter (Thermo Orion 5 Star) using a combined glass electrode (Orion 81–75). The pH meter was calibrated with buffers of pH 4.0 and 7.0 before any measurement.

The experiments for removal of manganese ions from dilute aqueous solutions by the addition of adsorbent (Co/Mo-LDH) masses 0.05, 0.10, 0.15, 0.20, 0.25, 0.30 and 0.35 g/L were carried out at different temperatures (298, 308 and 318 K), using distilled water and conical flasks (100 mL sample volume). After continuous stirring over a magnetic stirrer at about 160 rpm for a predetermined time intervals (15, 30, 45, 60, 75 and 90 min), the solid and solution were separated by centrifugation at 3000 rpm for 15 min and slightly dried at ambient temperature. Mn(II) concentration was determined by Spectro-photometer, LaMotte, model SMART Spectro, USA and the solid phase was analyzed. The contact time, allows the dispersion of adsorbent and metal ions to reach equilibrium conditions, as found during preliminary experiments.

3. Adsorption calculations

The amount of adsorption q_e (mg/g) and the percentage of removal were calculated by the following equations [16,17]:

$$q_e = (C_0 - C_e) \times V/m \tag{1}$$

$$\%\ \text{Removal} = (C_0 - C_e)/C_0 \times 100\% \tag{2}$$

where C_0 and C_e are the initial Mn(II) concentration and the concentration at equilibrium in mg/l, m is the mass of the adsorbent and V is the volume of solution.

Two adsorption isotherms models have been used to analyze the adsorption data equilibrium models to fit the experimental data by two equations [18]:

(i) Langmuir

$$C_e/q_e = 1/K_L b + C_e/b \tag{3}$$

where q_e (mg/g) is the equilibrium adsorption capacity and C_e (mg/l) is the equilibrium concentration. While, K_L (L/mg) and b (mg/g) are the Langmuir constants related to the sorption capacity and the adsorption energy, respectively.

(ii) Freundlich

$$\log q_e = \log K_F + 1/n \log C_e \tag{4}$$

while, K_F (L/mg) is the Freundlich constant and $1/n$ is the heterogeneity factor.

For a Langmuir type adsorption process, to determine if the adsorption is favorable or not, a dimensionless separation factor [19] is defined by:

$$R_L = 1/(1 + k_L C_o) \tag{5}$$

If $R_L > 1$, the isotherm is unfavorable; when $R_L = 1$, the isotherm is linear; in the range $0 < R_L < 1$, the isotherm is favorable; when $R_L = 0$, the isotherm is irreversible.

Adsorption kinetics is used to explain the adsorption mechanism and adsorption characteristics of Co/Mo-LDH. The pseudo-first-order and second-order kinetics equations [20,21] in linear forms are expressed as:

$$\log(q_e - q_t) = \log q_e - (k_1/2.303)t \tag{6}$$

$$t/q_t = 1/k_2\, q_e^2 + t/q_e \tag{7}$$

where q_t and q_e are the amounts of Co/Mo-LDH adsorbed at time t and at equilibrium, respectively; k_1 and k_2 are the pseudo-first-order and second-order rate constants for the adsorption process.

The thermodynamic parameters provide in-depth information on inherent energetic changes including Gibbs free energy change ($\Delta G°$), enthalpy change ($\Delta H°$), and entropy change ($\Delta S°$) for the adsorption process which are obtained by the following equations [22,23]:

$$\Delta G^{\circ} = -RT \ln b \tag{8}$$

$$\ln b = \Delta S^{\circ}/R - \Delta H^{\circ}/RT \tag{9}$$

where R is the ideal gas constant (kJ mol^{-1} K^{-1}), T is the temperature (K), and b is a Langmuir constant related to the adsorption energy (from the Langmuir isotherm).

4. Results and discussion

4.1. Characteristics of Co/Mo-LDH

4.1.1. XRD analysis

The XRD patterns of Co/Mo-LDH, before and after Mn(II) adsorption, are shown in Fig. 1. The patterns simply show the hydrotalcite structure of Co/Mo-LDH as the main structure (JCPDS file No. 22-700). The Co/Mo-LDH patterns were characterized by sharp, narrow and symmetric reflections at the lower 2 theta of basal (0 0 3), (0 0 6), and (0 0 9) planes in addition to asymmetric and broad reflections appearing at the higher 2 theta for non-basal (0 1 2), (0 1 5), and (0 1 8) planes. The repeatable diffractions by basal planes d(0 0 3) = 2d(0 0 6) = 3d(0 0 9) for Co/Mo-LDH reflect a fully crammed stacks of brucite-like layers ordered along axis c which resembles the thickness of the brucite-like layer and the interlayer space and its value is often determined as three times the spacing of (0 0 3) plane, so here it equals 2.04 nm since the Co/Mo-LDH XRD patterns have the main peak at 0.68 nm. This main peak value here is reduced if compared to 0.76 nm for the normal M^{2+}/M^{3+} LDHs and can be resolved by the formation of 4^+ charges in Co/Mo-LDH instead of 1^+ in case of the conventional LDHs and so stronger electrostatic interaction between the inorganic (Mo^{6+}) layer and the guest (CO_3^{2-}) anion [24,25].

4.1.2. FTIR spectroscopy

The IR-spectra of the prepared samples before and after the adsorption procedure are shown in Fig. 2. The spectra are coincident with those of ordinary LDHs intercalated with CO_3^{2-} anion [26,27]. The interlayer carbonate is proofed by the asymmetric stretching absorption band (υ3) of the CO_3^{2-}

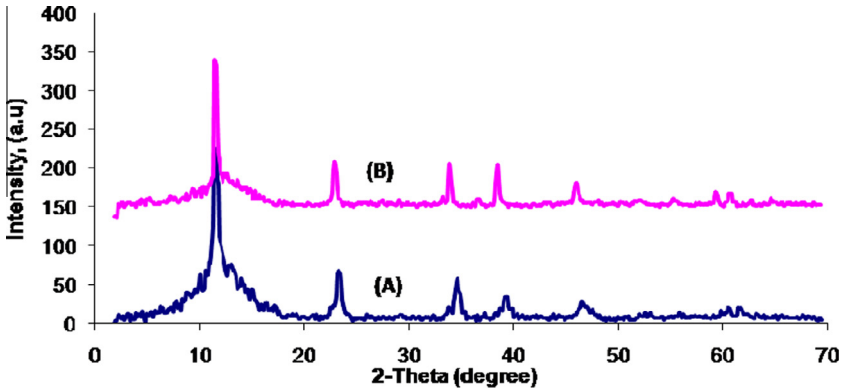

Figure 1 XRD patterns of Co/Mo-LDH: (A) before and (B) after Mn(II) adsorption.

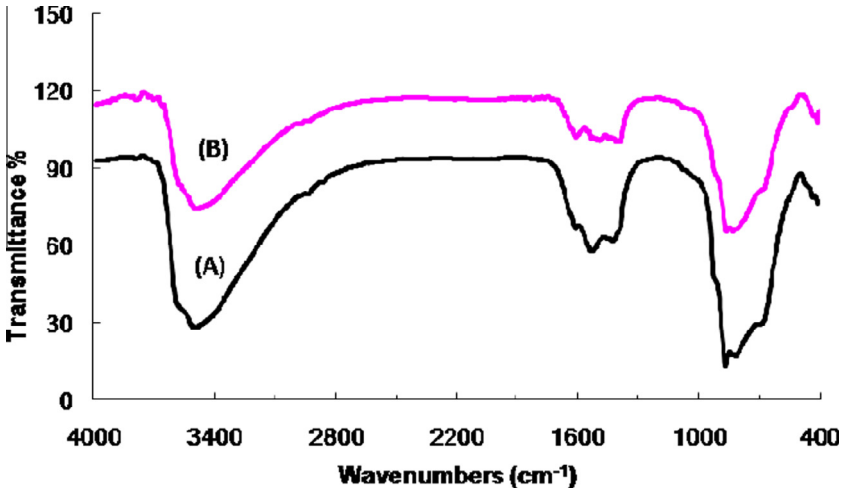

Figure 2 FT-IR spectra of Co/Mo-LDH: (A) before and (B) after Mn(II) adsorption.

near 1380 cm^{-1} with its attendant close to 1510 cm^{-1}. For free carbonate, this band is recorded at 1450 cm^{-1} but it splits and swings upon symmetry lowering which may be due to the constrained proportion in the interlayer space and the variable electrostatic interactions. The recorded broad band in region 3600–3200 cm^{-1} is related to the OH stretching mode of layer hydroxyl groups and of interlayer water molecules, and the broadness here may be due to hydrogen bridging [28–30], while the weak shoulder about 3000 cm^{-1} was due to the OH^{-} stretching mode of interlamellar water molecules coupled with the interlayer anions by hydrogen bridges. The weak band at 1600 cm^{-1} was for the bending band of water molecules [31], while the weak bands in the low frequency region 1000–500 cm^{-1} can be attributed to the O–Mo–O, Mo–O–Co and Co–OH in the parent Co/Mo-LDH [32,33].

4.1.3. SEM images

The SEM images of the Co/Mo-LDH before and after Mn(II) adsorption are shown in Fig. 3. The images exhibit a plate like morphology with fine crystallites which is usually related to the ordinary hydrotalcites with conservation of the Co/Mo-LDH structure before and after the adsorption procedure.

4.2. Initial solution pH

The effect of starting solution pH on the removal% of Mn(II) from solutions with an initial concentration of 145 mg/L, on 0.20 g/L of Co/Mo-LDH after 60 min is shown in Fig. 4. The data indicate that the amounts of Mn(II) adsorbed on Co/Mo-LDH decrease with decreasing pH for a starting solution pH $\leqslant$ 4, while for pH > 4, the removal seems to be pH-independent. The decrease in the Mn(II) removal in the low-pH range may be due to the dissolution of LDH in the low-pH solutions [34]. This was confirmed by the presence of Co and Mo in the final solution using the spectrophotometer analysis while, the lower adsorption at the higher pH range, may be due to the increasing competitive effect of OH-adsorption on LDH [35].

From Fig. 4, above pH 4, adsorption capacities increase with increasing pH, and reach its maximum value at pH 5 and then decrease. At pH 5, the adsorption capacities of Mn (II) on Co/Mo-LDH were 20.2, 26.75 and 38.1 mg/g at temperatures 298, 308 and 318 K, respectively. Then, the adsorption decreases and appears to reach a plateau in the pH range of $\geqslant$5–7.

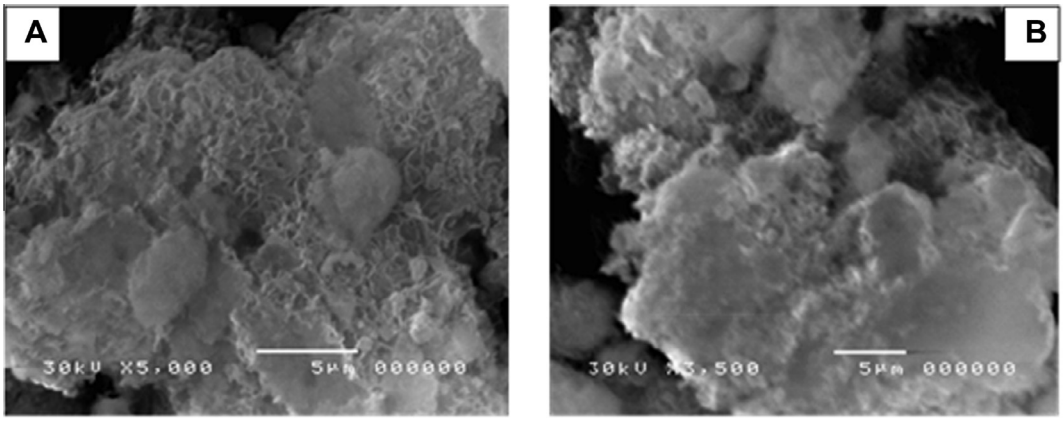

Figure 3 SEM images of Co/Mo-LDH: (A) before and (B) after Mn(II) adsorption.

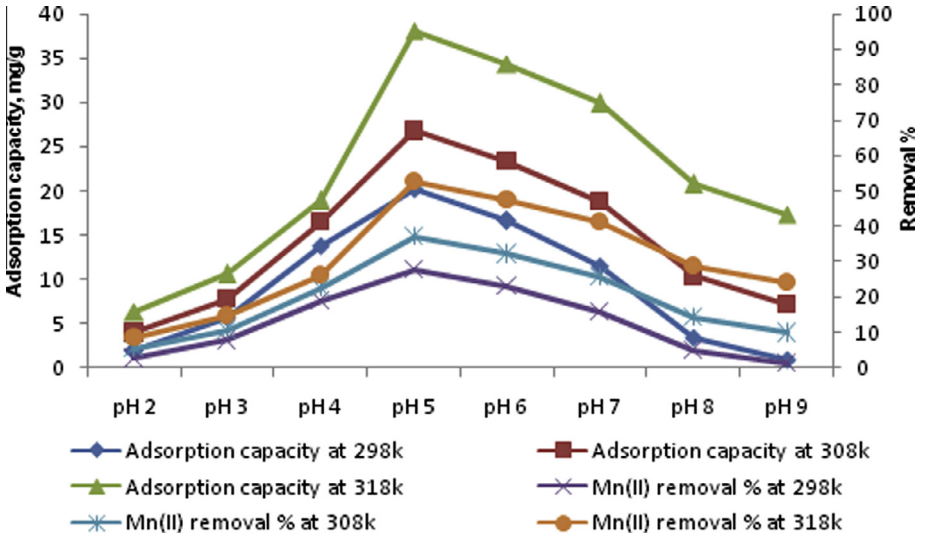

Figure 4 Effect of initial solution pH on the removal percentage and adsorption capacity of Co/Mo-LDH at different temperatures (initial Mn(II) concentration 145 mg/l, adsorbent mass 0.2 g/l, stirring rate 160 rpm, contact time 60 min).

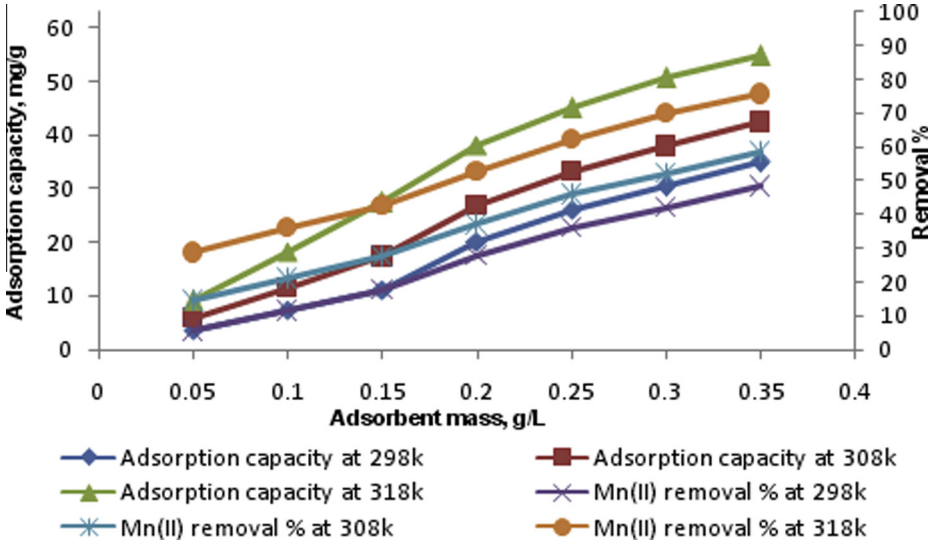

Figure 5 Adsorbent masses as a function of Mn(II) removal percentage and adsorption capacity of Co/Mo-LDH at different temperatures (initial Mn(II) concentration 145 mg/l, pH 5.0, stirring rate 160 rpm, contact time 60 min).

4.3. Adsorbent mass

Different amounts of Co/Mo-LDHs (0.05, 0.10, 0.15, 0.20, 0.25, 0.30 and 0.35 g/L) were added to a series of 100 mL of manganese solutions with initial concentration of 145 mg/L at pH 5 and stirring rate of 160 rpm for contact time 60 min to reach the equilibrium. Then the aqueous samples were filtered, and then the residual Mn(II) concentrations were analyzed. The effect of the LDH adsorbent mass on the Mn(II) adsorption in 145 mg/L solutions is shown in Fig. 5. For these experiments, the metal solutions containing the appropriate adsorbent dose were loaded in 100 mL snap-seal polyethylene bottles, which were then stirred at 160 rpm for 60 min. The mixture in each bottle was then centrifuged immediately, and the Mn(II) concentrations in the supernatant solutions were determined by a Spectrophotometer. At all temperatures, the first removal percentage of Mn(II) increased sharply with increasing the LDH dosage, at fixed initial adsorbate concentration (145 mg/L), and the loading capacity of the material decreases with increasing LDH dose at an adsorbent dose above 0.2 g/L [36]. Furthermore, at the higher LDH mass (0.35 g/L), the adsorption capacities of Mn(II) on Co/Mo-LDH are 36.95, 44.35 and 58.75 mg/g at temperatures 298, 308 and 318 K, respectively.

4.4. Initial Mn(II) concentration and adsorption isotherm

The effect of different Mn(II) concentrations was determined after experimental studies were carried out for a range of metal concentrations. A definite dosage of Co/Mo-LDH adsorbent (0.2 g/L) was added to a series of 100 mL of Mn(II) solutions with the different initial concentrations of 40, 55, 70, 85, 100, 115, 130 and 145 mg/L at pH 5.0, and stirring rate at 160 rpm for contact time 60 min to reach the equilibrium. The removal of Mn(II) shown in Fig. 6 indicates that Co/Mo-LDH apparently removes a considerable amount of Mn(II) from the aqueous solutions. The adsorption efficiency increases to a certain level, and saturates beyond a certain concentration. Saturation resulted when no more metal ions could be adsorbed on the surface of Co/Mo-LDH where the adsorption occurred. The experimental studies also showed that high efficiency for Mn(II) adsorption could be obtained over a relatively short period of up to 60 min. The removal with initial Mn(II) concentrations exhibits that the removal amounts are linearly proportional to the initial metal concentrations. However, the complete removal of Mn(II) was observed at initial concentration 40 mg/L at 308 K and at initial concentrations 40, 55 and 70 mg/L at 318 K. While, at temperature 298 K, only 63% from the initial concentration 40 mg/L was removed. Adsorption isotherm models are usually used to describe the interaction between the adsorbent and the adsorbate when the adsorption process reaches equilibrium, affording the most important parameter for designing a desired adsorption system. The equilibrium data were analyzed using the Langmuir and Freundlich equilibrium models in order to obtain the best fitting isotherm (Eqs. (3) and (4)). According to Fig. 7(a), K_F and n are the Freundlich constants, which represent sorption capacity and sorption intensity, respectively and they can be evaluated from the intercept and slope of the linear plot of log q_e versus log C_e and given in Table 1. While, from Fig. 7 (b), a line was obtained as the values of b as K_L can also be obtained by the slope and intercept of the line and given in Table 1.

The isotherm models of Mn(II) removal were studied by different initial concentrations ranging from 40 to 145 mg/L at different temperatures, 298, 308 and 318 K, a pH of 5, adsorbent mass of 0.2 g Co/Mo-LDH and after 60 min. Table 1 summarizes the Langmuir and Freundlich constants and the calculated coefficients. The results show that the linear correlation coefficients for Langmuir and Freundlich models are 0.965, 0.995 and 0.999 and 0.882, 0.867 and 0.802 at 298, 308 and 318 K, respectively. The higher regression coefficient R^2 for Langmuir model indicated that the Langmuir model fits

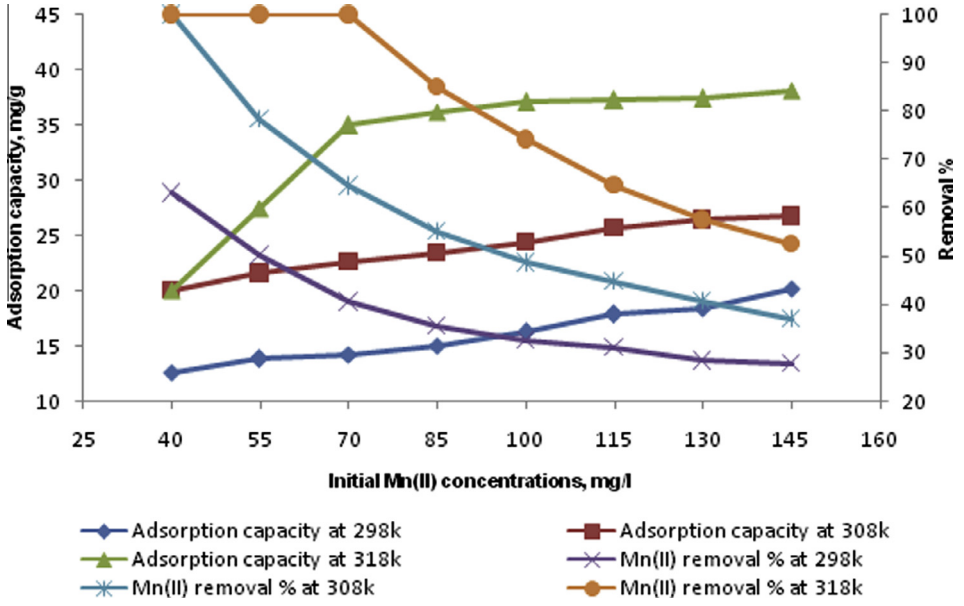

Figure 6 Effect of initial Mn(II) concentrations on the removal percentage and adsorption capacity of Co/Mo-LDH at different temperatures (pH 5.0, adsorbent mass 0.2 g/l, stirring rate 160 rpm, contact time 60 min).

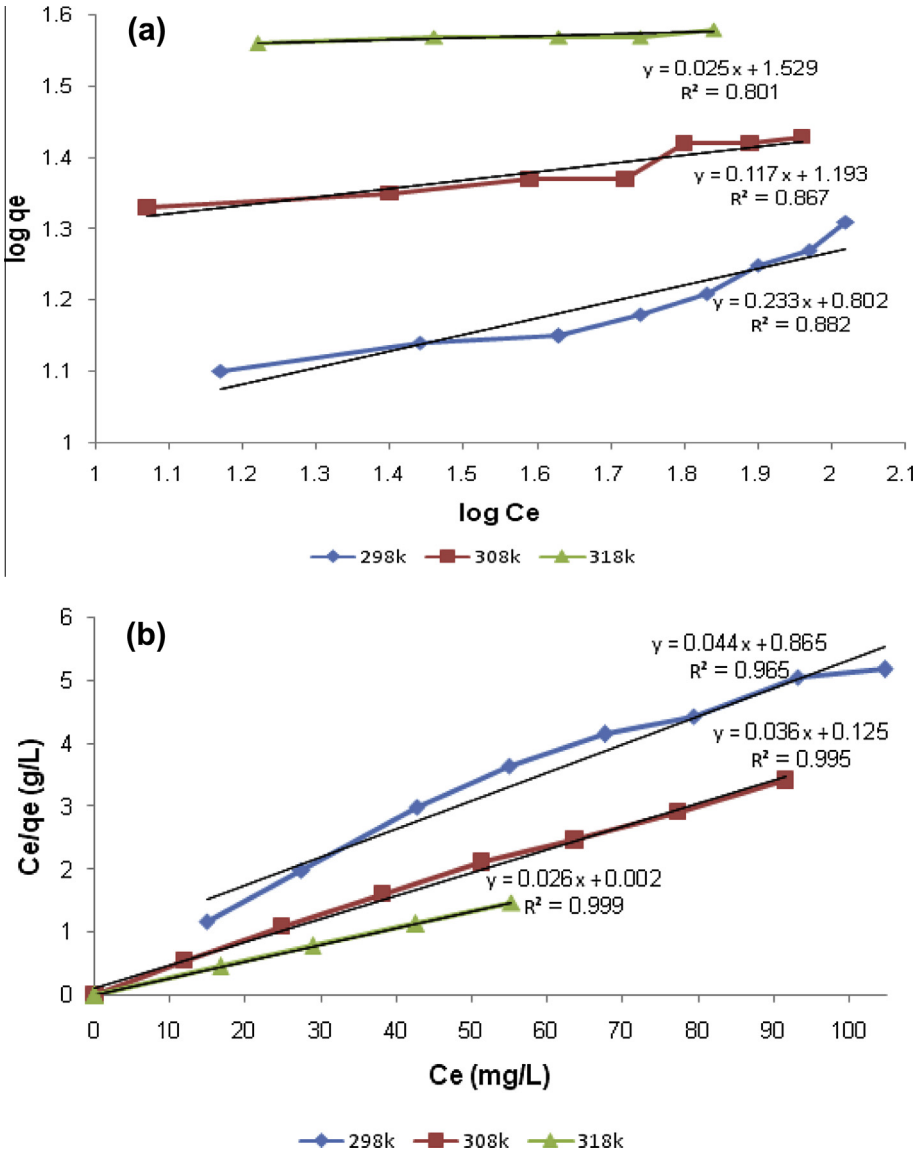

Figure 7 Isotherm models of: (a) Freundlich and (b) Langmuir for Mn(II) removal by Co/Mo-LDH at different temperatures (pH 5.0, adsorbent mass 0.2 g/l, stirring rate 160 rpm, contact time 60 min).

Table 1 Isotherm parameters for Mn(II) removal onto Co/Mo-LDH at different temperatures (pH 5.0, adsorbent mass 0.2 g/l, stirring rate 160 rpm, contact time 60 min).

T (K)	Langmuir isotherm model			Freundlich isotherm model		
	K_L (L/mg)	b (mg/g)	R^2	K_F (mg/g)	n	R^2
298	0.052	22.32	0.965	6.34	4.29	0.882
308	0.294	27.17	0.995	15.61	8.55	0.867
318	10.72	37.31	0.999	33.82	38.61	0.802

the experimental data better than the Freundlich one. Moreover, the Langmuir constant b values, which are a measure of the monolayer adsorption capacity of the adsorbent, were 22.32, 27.17 and 37.31 mg/g at 298, 308 and 318 K, respectively. The Langmuir constant, K_L, which denotes adsorption energy, was found to be 0.052, 0.294 and 10.72 L/mg at 298, 308 and 318 K, respectively. Therefore, to determine if the adsorption is favorable or not, we used a dimensionless separation factor equation (Eq. (5)), the dimensionless parameter, R_L, which is a measure of adsorption favorability was 0.325–0.117, 0.078–0.029 and 0.0023–0.0006 at 298, 308 and 318 K, respectively, (i.e., $0 < R_L < 1$) suggesting that the adsorption of Mn(II) on Co/Mo-LDH is favorable, as observed experimentally.

4.5. Contact time and adsorption kinetics

Fig. 8 shows the effect of contact time on the adsorption capacity and % removal of Mn(II) 145 mg/L initial concentration onto 0.2 g/L Co/Mo-LDH at pH 5, stirring rate of 160 rpm and different temperatures, 298, 308 and 318 K. It can be seen from Fig. 8 that the adsorption rate is considerably

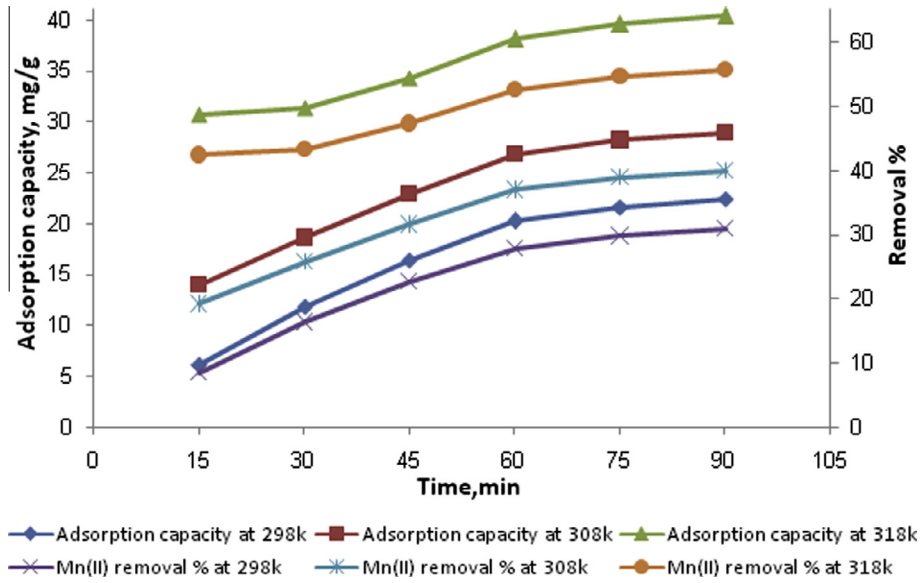

Figure 8 Effect of contact time on the Mn(II) removal percentage and adsorption capacity of Co/Mo-LDH at different temperatures (initial concentration 145 mg/l, pH 5.0, adsorbent mass 0.2 g/l, stirring rate 160 rpm).

Table 2 Kinetic parameters of the pseudo-first- and pseudo-second-order models for the Mn(II) adsorption onto Co/Mo-LDH at different temperatures (initial Mn(II) concentration 145 mg/l, pH 5.0, adsorbent mass 0.2 g/l, stirring rate 160 rpm).

T (K)	Pseudo-first-order model			Pseudo-second-order model		
	k_1 (min^{-1})	q_e (mg/g)	R^2	k_2 (g mg^{-1} L min^{-1})	q_e (mg/g)	R^2
298	7.4×10^{-3}	45.78	0.913	2.28×10^{-4}	47.62	0.920
308	0.0134	29.60	0.968	8.82×10^{-4}	38.76	0.993
318	0.0166	20.10	0.973	1.96×10^{-3}	45.05	0.995

fast within the first 30 min, then gradually slowed down and thereafter, the adsorption equilibrium is reached at 60 min.

The fast Mn(II) removal rate in the beginning is attributed to the rapid diffusion of Mn(II) from the solution to the external surfaces of Co/Mo-LDH. The subsequent slow adsorption process is attributed to the longer diffusion range of Mn(II) into the inner-sphere of Co/Mo-LDH or the ion-exchange in the inner surface of Co/Mo-LDH. Such slow diffusion will lead to a slow increase in the adsorption curve at later stages [37]. Moreover, the initial rapid adsorption may be due to an increased number of available sites at the initial stage. The increase in concentration gradient tends to increase Mn(II) adsorption rate within the initial 30 min. As time proceeds, the concentration gradients become reduced owing to the accumulation of more than 11.8, 18.6 and 31.35 mg of Mn(II) adsorbed per gram of Co/Mo-LDH surface sites after 30 min, leading to the maximum adsorption capacities 20.2, 26.75 and 38.1 mg/g after 60 min and then at the later time (90 min), the adsorption rate became constant 22.35, 28.95 and 40 mg/g at 298, 308 and 318 K, respectively.

To evaluate the adsorption kinetics of Mn(II) ions on Co/Mo-LDH, the pseudo-first-order and pseudo-second-order models (Eqs. (6) and (7)) were applied to analyze the experimental data. The kinetic model parameters were obtained from fitting results and presented in Table 2. From the fit curve shown in Fig. 9 and the relative coefficient, it can be seen that the pseudo-second-order model fits the adsorption of Mn(II) on Co/Mo-LDH better than the pseudo-first-order model.

In this study, as illustrated in Fig. 9, the slopes and intercepts of the plot of t versus log ($q_e - q_t$) and t/q_t were used to determine the rate constants k_1 and k_2 and the equilibrium adsorption density q_e of the pseudo-first-order and pseudo-second-order, respectively, Table 2. The correlation coefficients for the pseudo-first-order model (R^2 = 0.913, 0.968 and 0.973) were lower than that of the pseudo-second-order (R^2 = 0.920 0.993 and 0.995) at 298, 308 and 318 K, respectively. This suggests that the pseudo-first-order equation might not be sufficient to depict the kinetics of Mn(II) on the Co/Mo-LDH and the kinetic parameters for the pseudo-second-order model best described by the pseudo-second order model.

4.6. Adsorption mechanism

While the Langmuir model assumes that the adsorption occurs on a homogeneous surface by monolayer coverage, with uniform binding sites, equivalent sorption energies and no interactions between adsorbed species, the Freundlich isotherm is an empirical equation assuming that the adsorption process takes place on heterogeneous surfaces, and adsorption

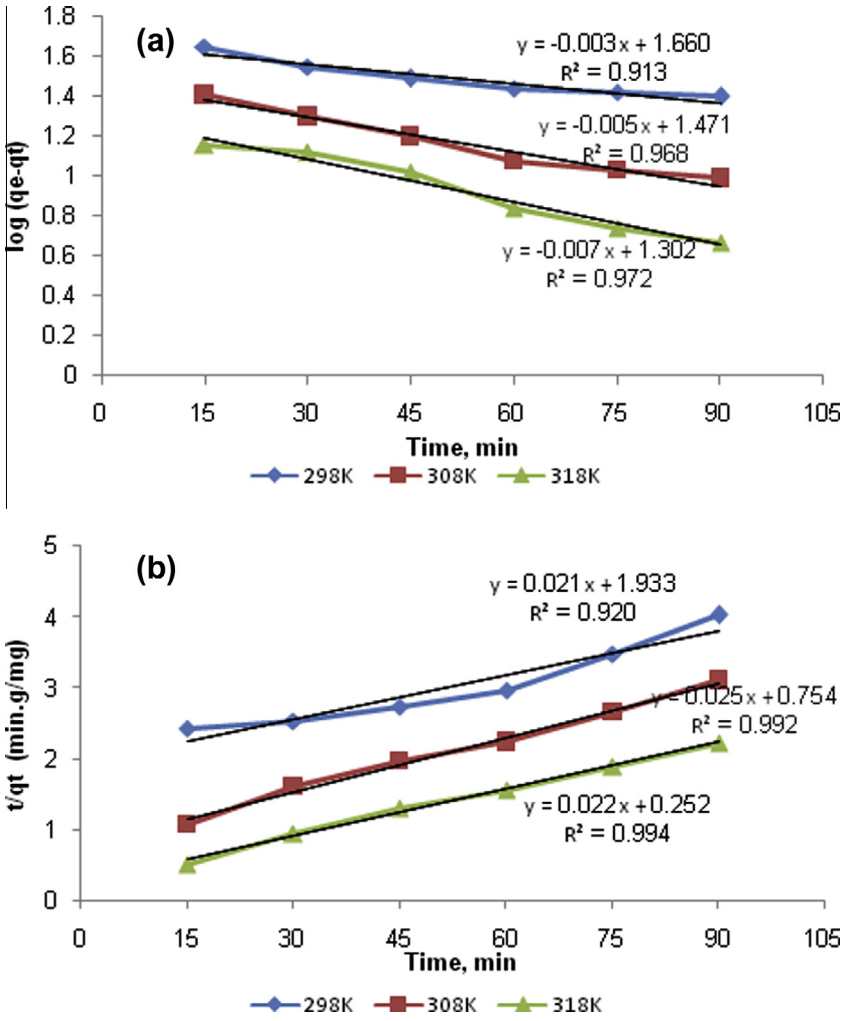

Figure 9 Adsorption kinetics of: (a) pseudo-first-order and (b) pseudo-second-order models for the Mn(II) adsorption by Co/Mo-LDH at different temperatures (initial Mn(II) concentration 145 mg/l, pH 5.0, adsorbent mass 0.2 g/l, stirring rate 160 rpm).

capacity is related to the concentration of the adsorbate at equilibrium. In other words, the experimental data well fitted to Langmuir equation confirming that the binding energy on the whole surface of Co/Mo-LDH is uniform. This means that, the whole surface has identical adsorption activity and therefore the adsorbed manganese ions do not interact or compete with each other, and they are adsorbed by forming almost complete monolayer coverage of the Co/Mo-LDH particles. This phenomenon also shows that chemisorption is the principal uptake mechanism in adsorption process [38].

The better understanding of the mechanism of manganese adsorption was illustrated by adsorption kinetics. When the pseudo-second-order model considers the rate-limiting step as the formation chemisorptive bond involving sharing or exchange of electrons between adsorbate and the adsorbent [39], the above results obtained consistently suggests that the rate-determining step may be chemical adsorption and the adsorption behavior may involve the valence forces through sharing electrons between the Mn(II) ions and adsorbents [40,41].

Therefore, the above results obtained consistently suggests that mechanism of Mn(II) adsorption on Co/Mo-LDH and the higher adsorption capacity of the Co/Mo-LDH is explained by the formation of 4^+ surface charges between Co^{2+} and Mo^{6+} which means formation of a highly energetic surface layers as detected by XPS [14].

4.7. Temperature and thermodynamics

All experiments in this study were carried out at different temperatures 298, 308, and 318 K. The adsorption capacity of Mn (II) onto Co/Mo-LDH as a function of initial Mn(II) concentration and contact time is shown in Figs. 6 and 8, respectively. The thermodynamic parameters were calculated and the nature of the adsorption processes was determined at different temperatures and the adsorption capacity of Mn(II) for Co/Mo-LDH increased with increasing the temperature.

From Eq. (8), the negative values for the Gibbs free energy ($\Delta G°$) for all different temperatures were −7.69, −8.44 and −9.55 kJ mol^{-1}, respectively, showing that the adsorption process is spontaneous and the degree of spontaneity of the reaction increased with the increase in the temperature and the value of $\Delta G°$ becomes more negative indicating that higher temperature facilitates the adsorption of Mn(II) on Co/Mo-LDH due to a greater driving force of adsorption.

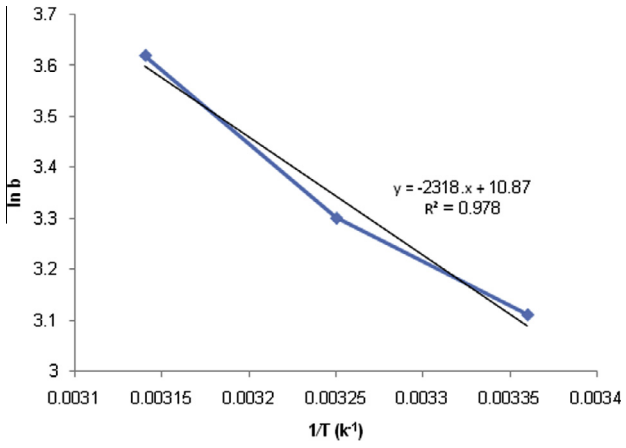

Figure 10 Plot of the Langmuir isotherm constant ($\ln b$) vs. temperature ($1/T$) (the thermodynamic parameters in Table 3 are determined from this graph).

Table 3 Thermodynamic constants for the Mn(II) adsorption onto Co/Mo-LDH at different temperatures (pH 5.0, adsorbent mass 0.2 g/l, stirring rate 160 rpm, contact time 60 min).

T (K)	$\ln b$	$\Delta G°$ (kJ mol^{-1})	$\Delta H°$ (kJ mol^{-1})	$\Delta S°$ (kJ mol^{-1} K^{-1})	R^2
298	3.11	−7.69	19.24	0.09	0.979
308	3.30	−8.44			
318	3.62	−9.55			

Eq. (9) represents the enthalpy ($\Delta H°$) and the entropy ($\Delta S°$) changes that were calculated from a plot of $\ln b$ (from the Langmuir isotherm) vs. $1/T$, Fig. 10. The results of these thermodynamic calculations are shown in Table 3. The positive value of $\Delta H°$ (19.24 kJ mol^{-1}) suggests that the interaction of Mn(II) adsorbed by Co/Mo-LDH is endothermic process. Table 3, also shows that the $\Delta S°$ value (0.09 kJ mol^{-1} K^{-1}) was positive which revealed the increased randomness at the solid–solution interface during the process of adsorption [42–44].

5. Conclusions

The present study shows that the synthesized Co/Mo-LDH is a suitable adsorbent for the Mn(II) removal from aqueous solutions. The behavior of adsorption process was studied as a function of contact time, initial Mn(II) concentration, solution pH and adsorbent mass. The adsorption processes were rapidly carried out at different temperatures (298, 308 and 318 K) and constant stirring rate. The solution pH range of 4–7 has the most significant effect on the adsorption capacity and the adsorption capacity increased with increasing the temperature. The experimental data well fitted to Langmuir equation confirming the monolayer coverage of Mn(II) solution onto layered double hydroxide adsorbent. The main mechanism controlling the adsorption of Mn(II) onto the LDH may be the ion exchange with carbonate and the ligand exchange with layer OH group. Kinetically, the adsorption process followed the pseudo-second-order mechanism that considers the rate-limiting step as the formation of chemisorptive bond involving sharing or exchange of electrons between the Mn(II) and LDH. Also, the thermodynamic parameters of the adsorption such as Gibbs free energy, entropy, and enthalpy were discussed and the results demonstrate that the adsorption process is spontaneous and endothermic.

References

[1] P. Roccaro, C. Barone, G. Mancini, F.G.A. Vagliasindi, Desalination 210 (2007) 205–214, http://dx.doi.org/10.1016/j.desal.2006.05.045.
[2] WHO, Guideline for Drinking Water Quality, Health Criteria and Other Supporting Information, vol. 1, third ed., Geneva, 2004.
[3] European Union, Richtlinie 98/83/EG des Rates, 1998.
[4] U.S. EPA, Office of water, National secondary drinking water regulations, In Code of Federal Regulations, 2001, pp. 612–614.
[5] S.C. Homoncik, A.M. MacDonald, K.V. Heal, B.É.Ó. Dochartaigh, B.T. Ngwenya, Sci. Total Environ. 408 (2010) 2467–2473, http://dx.doi.org/10.1016/j.scitotenv.2010.02.017.
[6] A.G. Tekerlekopoulou, D.V. Vayenas, Desalination 210 (2006) 225–235, http://dx.doi.org/10.1016/j.desal.2006.05.047.
[7] A. Voorinen, Water Sci. Technol. 20 (1988) 249–259.
[8] A.B. Jusoh, W.H. Cheng, W.M. Low, N. Ali, M.J. Noor, Desalination 182 (2005) 347–353, http://dx.doi.org/10.1016/j.desal.2005.03.022.
[9] V.A. Pacini, A.M. Ingallinella, G. Sanguinetti, Water Res. 39 (2005) 4463–4475, http://dx.doi.org/10.1016/j.watres.2005.08.027.
[10] I.A. Katsoyiannis, A.I. Zouboulis, Water Res. 38 (2004) 1922–1932, http://dx.doi.org/10.1016/j.watres.2004.01.014.
[11] S. Zhang, F. Cheng, Z. Tao, F. Gao, J. Chen, J. Alloys Compd. 426 (2006) 281–285, http://dx.doi.org/10.1016/j.jallcom.2006.01.095.
[12] G. Yanwei, Z. Zhiliang, Q. Yanling, Z. Jianfu, J. Hazard. Mater. 239–240 (2012) 279–288, http://dx.doi.org/10.1016/j.jhazmat.2012.08.075.
[13] N.N. Das, J. Konar, M.K. Mohanta, S.C. Srivastava, J. Colloid Interface Sci. 270 (2004) 1–8, http://dx.doi.org/10.1016/S0021-9797(03)00400-4.
[14] A.A. Bakr, M.S. Mostafa, Gh. Eshaq, M.M. Kamel, Desalin. Water Treat. (2014) 1–8, http://dx.doi.org/10.1080/19443994.2014.934729.
[15] M.S. Mostafa, A.A. Bakr, Gh. Eshaq, M.M. Kamel, Desalin. Water Treat. (2014) 1–9, http://dx.doi.org/10.1080/19443994.2014.934725.
[16] A. Legrouri, M. Lakraimi, A. Barroug, A.D. Roy, J.P. Besse, Water Res. 39 (2005) 3441–3448, http://dx.doi.org/10.1016/j.watres.2005.03.036.
[17] A.A. Bakr, Y.M. Moustafa, M.M.H. Khalil, M.M. Yehia, E.A. Motawea, Can. J. Chem. 92 (2014) 1–9, http://dx.doi.org/10.1139/cjc-2014-0282.
[18] T. Hartono, S. Wang, Q. Ma, Z. Zhu, J. Colloid Interface Sci. 333 (2009) 114–119, http://dx.doi.org/10.1016/j.jcis.2009.02.005.
[19] K.R. Hall, L.C. Eagleton, A. Acrivos, T. Vermeulen, Ind. Eng. Chem. Fundam. 5 (1966) 212–223, http://dx.doi.org/10.1021/i160018a011.
[20] E. Bulut, M. Özacar, I.A. Sengil, J. Hazard. Mater. 154 (2008) 613–622, http://dx.doi.org/10.1016/j.jhazmat.2007.10.071.
[21] Y.S. Ho, G. McKay, Process Biochem. 34 (1999) 451–465.
[22] Z. Reddad, C. Gerente, Y. Andres, P.L. Le Cloirec, Environ. Sci. Technol. 36 (2002) 2067–2073, http://dx.doi.org/10.1021/es0102989.
[23] Y. Liu, Sep. Purif. Technol. 61 (2008) 229–242, http://dx.doi.org/10.1016/j.seppur.2007.10.002.
[24] V.R.L. Constantino, T.J. Pinnavaia, Inorg. Chem. 34 (1995) 883–892, http://dx.doi.org/10.1021/ic00108a020.

[25] S.K. Yun, T.J. Pinnavaia, Chem. Mater. 7 (1995) 348–354, http://dx.doi.org/10.1021/cm00050a017.
[26] M.J. Hernandez-Moreno, M.A. Ulibarri, J.L. Rendon, C.J. Serna, Phys. Chem. Miner. 12 (1985) 34–38.
[27] J.T. Kloprogge, R.L. Frost, J. Solid State Chem. 146 (1999) 506–515.
[28] F. Cavani, F. Trifiro, A. Vaccari, Catal. Today 11 (1991) 173–301, http://dx.doi.org/10.1016/0920-5861(91)80068-K.
[29] A. Vaccari, Appl. Clay Sci. 14 (1999) 161–198.
[30] F.M. Labajos, V. Rives, M.A. Ulibarri, J. Mater. Sci. 27 (1992) 1546–1552.
[31] J. Perez-Ramireez, G. Mul, F. Kapteijn, J.A. Moulijn, J. Mater. Chem. 11 (2001) 821–830, http://dx.doi.org/10.1039/B009320N, Paper.
[32] N. Nakamoto, Infrared and Raman Spectra of Inorganic and Co-ordination Compounds, fourth ed., John Wiley & Sons, New York, NY, 1986.
[33] A.M. El-Toni, S. Yin, T. Sato, Mater. Chem. Phys. 89 (2005) 154–158, http://dx.doi.org/10.1016/j.matchemphys.2004.08.029.
[34] M.C. Hermosin, I. Pavlovic, M.A. Ulibarri, J. Cornejo, Water Res. 30 (1996) 171–177.
[35] L. Yang, Z. Shahrivari, P. Liu, M. Sahimi, T. Tsotsis, Ind. Eng. Chem. Res. 44 (2005) 6804–6815, http://dx.doi.org/10.1021/ie049060u.
[36] D.P. Das, J. Das, K. Parida, J. Colloid Interface Sci. 261 (2003) 213–220, http://dx.doi.org/10.1016/S0021-9797(03)00082-1.
[37] M.H. Al-Qunaibit, W.K. Mekhemer, A.A. Zaghloul, J. Colloid Interface Sci. 283 (2005) 316–321, http://dx.doi.org/10.1016/j.jcis.2004.09.022.
[38] Y.T. Zhou, H.L. Nie, C. Branford-White, Z.Y. He, L.M. Zhu, J. Colloid Interface Sci. 330 (2009) 29–37, http://dx.doi.org/10.1016/j.jcis.2008.10.026.
[39] C. Chen, J.L. Wang, J. Hazard. Mater. 151 (2008) 65–70, http://dx.doi.org/10.1016/j.jhazmat.2007.05.046.
[40] A.K. Bhattacharya, T.K. Naiya, S.N. Mondal, S.K. Das, Chem. Eng. J. 137 (2008) 529–541, http://dx.doi.org/10.1016/j.cej.2007.05.021.
[41] L.M. Zhou, J.Y. Jin, Z.R. Liu, X.Z. Liang, C. Shang, J. Hazard. Mater. 185 (2011) 1045–1052, http://dx.doi.org/10.1016/j.jhazmat.2010.10.012.
[42] L. Ai, C. Zhang, Z. Chen, J. Hazard. Mater. 192 (2011) 1515–1524, http://dx.doi.org/10.1016/j.jhazmat.2011.06.068.
[43] K.H. Goh, T.T. Lim, Z. Dong, Environ. Sci. Technol. 43 (2009) 2537–2543, http://dx.doi.org/10.1021/es802811n.
[44] M. Dakiky, M. Khamis, A. Manassra, Adv. Environ. Res. 6 (2002) 533–540, http://dx.doi.org/10.1016/S1093-0191(01)00079-X.